MNRAS 000, 1–17 (2019) Preprint 4 November 2019 Compiled using MNRAS LATEX style file v3.0

Swirls of FIRE: Spatially Resolved Gas Velocity Dispersions and Star Formation Rates in FIRE-2 Disk Environments

Matthew E. Orr[1]★, Christopher C. Hayward[2], Anne M. Medling[3,4]†, Philip F. Hopkins[1], Norman Murray[5], Jorge L. Pineda[6], Claude-André Faucher-Giguère[7], Dušan Kereš[8], and Kung-Yi Su[1,2]

[1] *TAPIR, Mailcode 350-17, California Institute of Technology, Pasadena, CA 91125, USA*
[2] *Center for Computational Astrophysics, Flatiron Institute, 162 Fifth Avenue, New York, NY 10010, USA*
[3] *Ritter Astrophysical Research Center University of Toledo Toledo, OH 43606, USA*
[4] *Research School for Astronomy & Astrophysics Australian National University Canberra, ACT 2611, Australia*
[5] *Canadian Institute for Theoretical Astrophysics, 60 St George Street, University of Toronto, ON M5S 3H8, Canada*
[6] *Jet Propulsion Laboratory, California Institute of Technology, 4800 Oak Grove Drive, Pasadena, CA 91109-8099, USA*
[7] *Department of Physics and Astronomy and CIERA, Northwestern University, 2145 Sheridan Road, Evanston, IL 60208, USA*
[8] *Department of Physics, Center for Astrophysics and Space Science, University of California at San Diego, 9500 Gilman Drive, La Jolla, CA 92093, USA*

Accepted XXX. Received YYY; in original form ZZZ

ABSTRACT

We study the spatially resolved (sub-kpc) gas velocity dispersion (σ)–star formation rate (SFR) relation in the FIRE-2 (Feedback in Realistic Environments) cosmological simulations. We specifically focus on Milky Way mass disk galaxies at late times. In agreement with observations, we find a relatively flat relationship, with $\sigma \approx 15 - 30$ km/s in neutral gas across 3 dex in SFRs. We show that higher dense gas fractions (ratios of dense gas to neutral gas) and SFRs are correlated at constant σ. Similarly, lower gas fractions (ratios of gas to stellar mass) are correlated with higher σ at constant SFR. The limits of the σ-$\Sigma_{\rm SFR}$ relation correspond to the onset of strong outflows. We see evidence of "on-off" cycles of star formation in the simulations, corresponding to feedback injection timescales of 10-100 Myr, where SFRs oscillate about equilibrium SFR predictions. Finally, SFRs and velocity dispersions in the simulations agree well with feedback-regulated and marginally stable gas disk (Toomre's $Q = 1$) model predictions, and the data effectively rule out models assuming that gas turns into stars at (low) constant efficiency (i.e., 1% per free-fall time). And although the simulation data do not entirely exclude gas accretion/gravitationally powered turbulence as a driver of σ, it appears to be strongly subdominant to stellar feedback in the simulated galaxy disks.

Key words: galaxies: ISM, evolution, formation, kinematics and dynamics, star formation, ISM: kinematics and dynamics

Table 1. Summary of $z \approx 0$ properties of the FIRE-2 Milky Way-like galaxies used in this work

Name	$\log(\frac{M_\star}{M_\odot})$	$\log(\frac{M_{gas}}{M_\odot})$	$\frac{R_{\star,1/2}}{kpc}$	$\frac{R_{gas,1/2}}{kpc}$	$\frac{v_c}{km/s}$ *
m12b	10.8	10.3	2.7	9.4	266
m12c	10.7	10.3	3.4	8.6	232
m12f	10.8	10.4	4.0	11.6	248
m12i	10.7	10.3	2.9	9.8	232
m12m	10.9	10.4	5.6	10.2	283
m12r	10.2	10.0	4.7	9.9	156
m12w	10.6	9.8	3.1	3.1	244

Note: all quantities measured within a 30 kpc cubic aperture.
*Circular velocities evaluated at $R_{gas,1/2}$.

Гравитация + гидродинамика
FIRE-2 (Feedback In Realistic Environment)

$$\tilde{Q}_{gas} \equiv \frac{\sqrt{2}\sigma_z \Omega}{\pi G(\Sigma_{gas} + \gamma\Sigma_\star)},$$

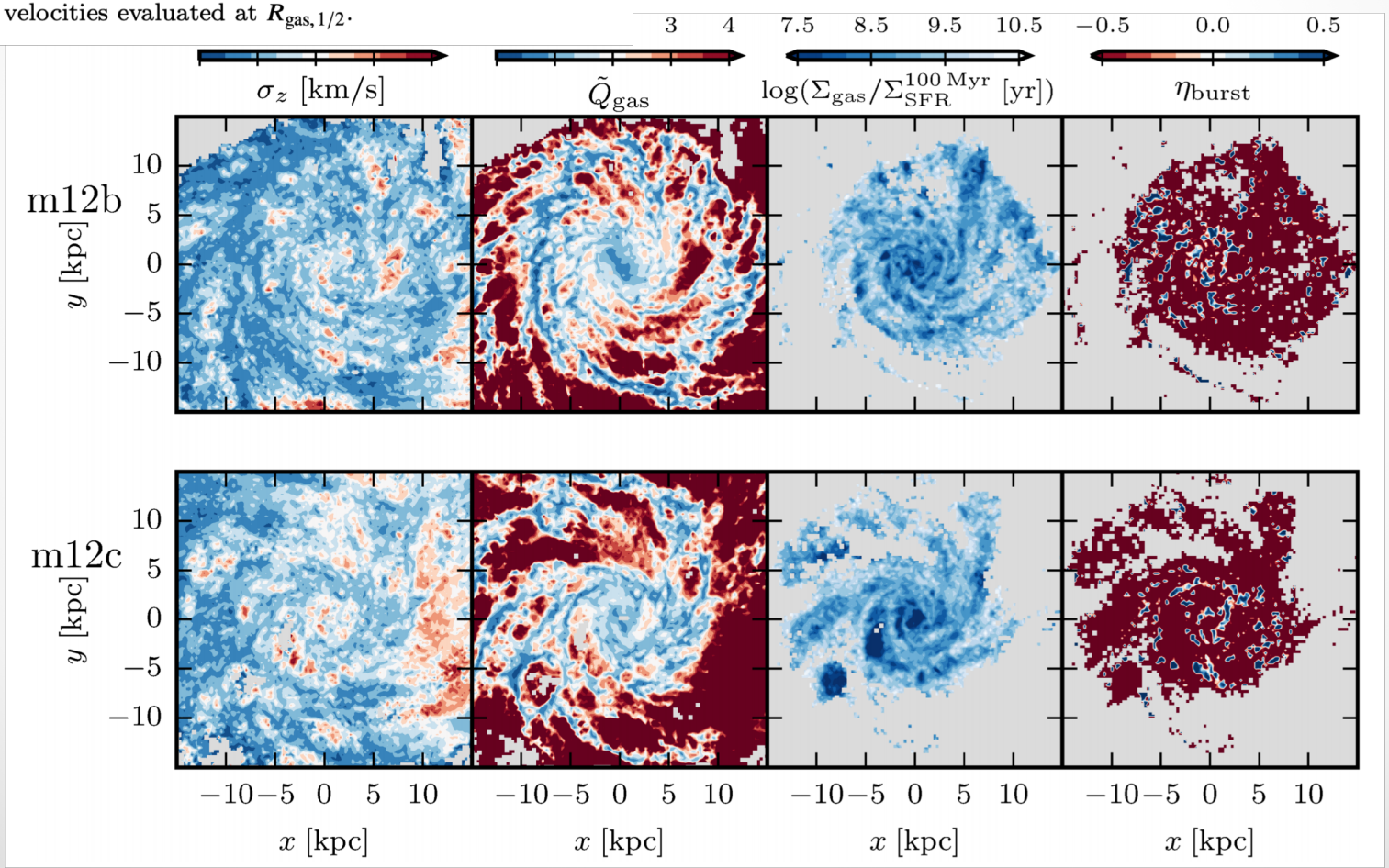

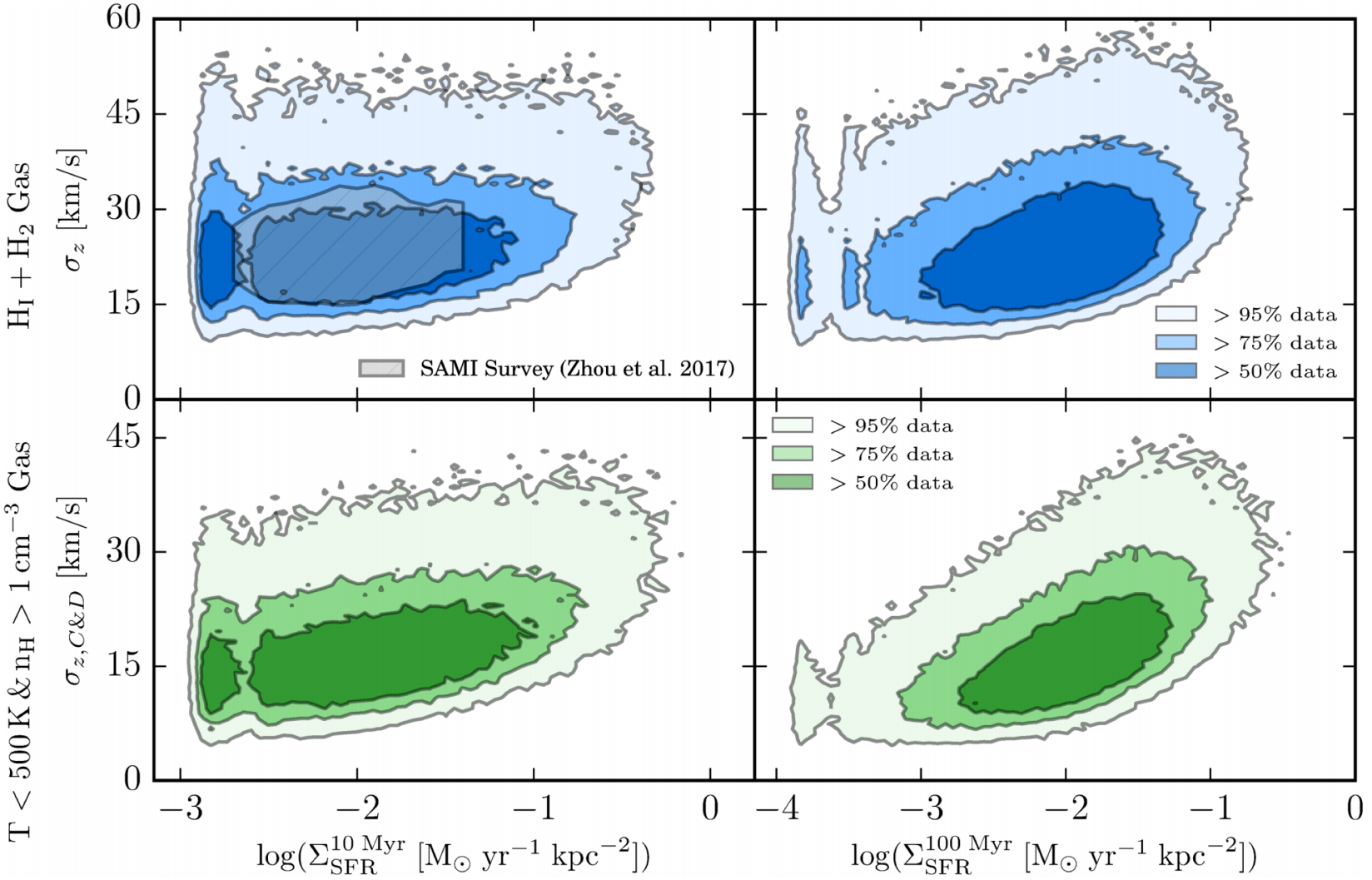

Figure 2. Distributions of spatially resolved (750 pc pixel size) line-of-sight gas velocity dispersions (σ_z) and SFR surface densities for various gas and SFR tracers in the Milky Way-mass FIRE simulations for $z \lesssim 0.1$. Gas velocity dispersions are the mass-weighted standard deviation of the line-of-sight velocities in gas, intentionally including inflow, outflow, non-circular galactic motions, etc. Data are stacked together from all individual m12 galaxy simulations (see, Fig. A2). Filled contours indicate 95, 70, 50-percentile inclusion regions for the simulation data. Velocity dispersions in neutral gas as a function of 10 Myr-averaged SFR are compared with observational data from Zhou et al. (2017). Across ~ 3 dex in SFRs, gas velocity dispersions are nearly constant, with a rising lower envelope of dispersions at a given SFR. The velocity dispersions for the cold and dense gas ($T < 500$ K and $n > 1$ cm^{-3}, *bottom row*) are lower than for neutral gas (atomic + molecular hydrogen, *top row*), indicating the dynamically colder state of the dense molecular component of the ISM. Tracers with longer averaging timescales (100 Myr vs. 10 Myr, *right and left columns, respectively*) are able to trace the relation to lower star formation rates and gas velocity dispersions, showing that there is a trend, but that it is very weak and only apparent over longer averaging timescales.

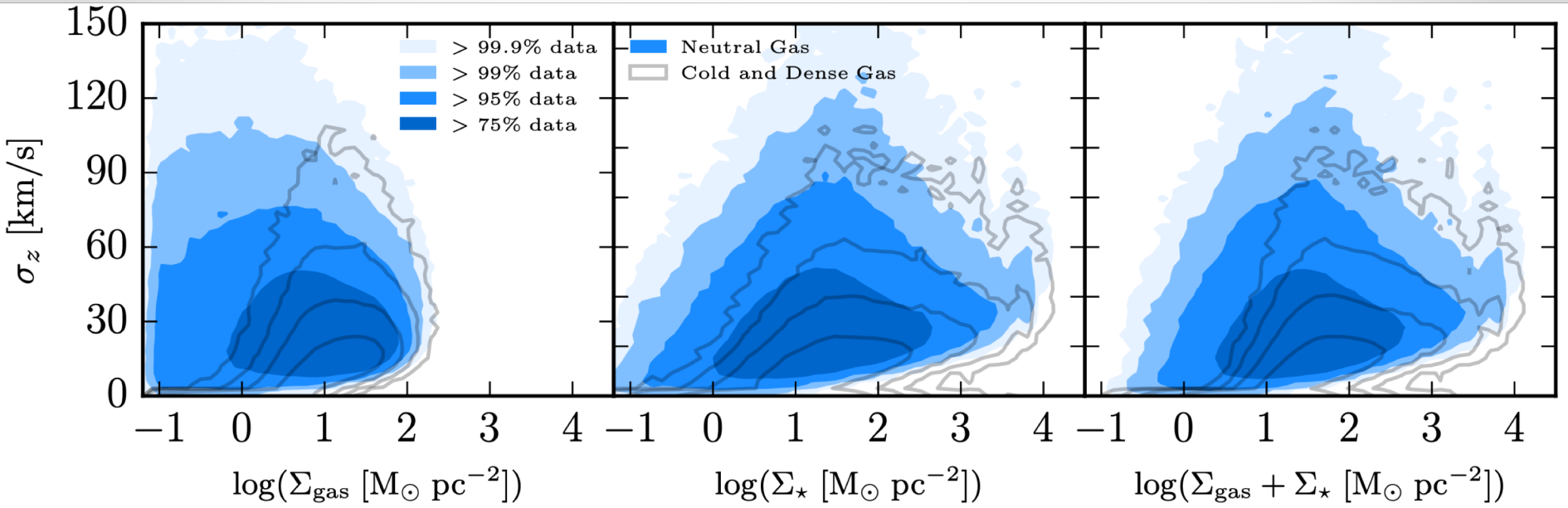

Figure 3. Distribution of σ_z (as Fig. 2) versus gas surface density ($\Sigma_{\rm gas}$), stellar surface density ($\Sigma_\star$), and total surface density ($\Sigma_{\rm gas}+\Sigma_\star$). Unfilled contours indicate velocity dispersions and gas surface densities of the cold and dense ($T < 500$ K and $n > 1$ cm^{-3}) component, with identical data inclusion percentages. We do not plot below below $\Sigma_{\rm gas} = 0.1$ M$_\odot$ pc^{-2} to ensure at least ~ 10 gas elements per pixel for calculating σ_z. **Left:** As neutral gas surface densities exceed ~few M$_\odot$ pc^{-2}, the ISM transitions to a predominantly molecular form, and velocity dispersions rise in the cold ISM component. **Center:** Largest scatter in velocity dispersions occurs for $\log\Sigma_\star \sim 1.5$. **Right:** Total surface density–velocity dispersion distribution is very similar to the stellar surface density–velocity distribution in neutral gas, but for cold and dense gas there is a steeper rise in dispersions (and generally cold gas content) around total surface densities of ~10 M$_\odot$ pc^{-2}. Generally higher neutral gas surface densities have a lower scatter to high dispersions, whereas the cold and dense gas velocity dispersions consistently rise with increasing gas and stellar surface densities.

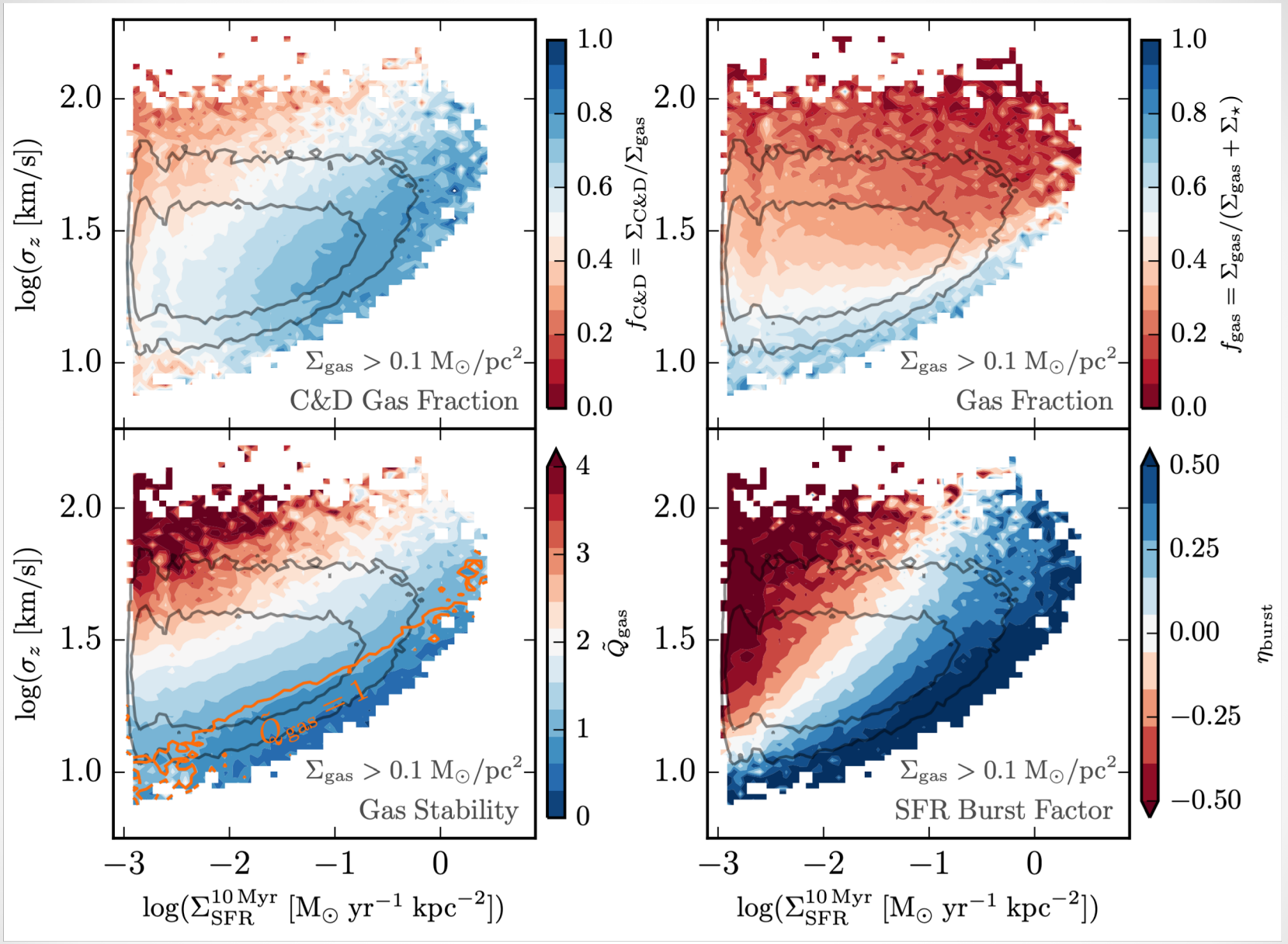
log(σz [km/s])
2.0
1.5
1.0
Σgas > 0.1 M⊙/pc²
C&D Gas Fraction
fC&D = ΣC&D/Σgas
1.0
0.8
0.6
0.4
0.2
0.0
Σgas > 0.1 M⊙/pc²
Gas Fraction
fgas = Σgas/(Σgas + Σ⋆)
1.0
0.8
0.6
0.4
0.2
0.0
log(σz [km/s])
2.0
1.5
1.0
Σgas > 0.1 M⊙/pc²
Gas Stability
Qgas = 1
Q̃gas
4
3
2
1
0
Σgas > 0.1 M⊙/pc²
SFR Burst Factor
ηburst
0.50
0.25
0.00
−0.25
−0.50
−3
−2
−1
0
log(Σ10 Myr SFR [M⊙ yr−1 kpc−2])
−3
−2
−1
0
log(Σ10 Myr SFR [M⊙ yr−1 kpc−2])

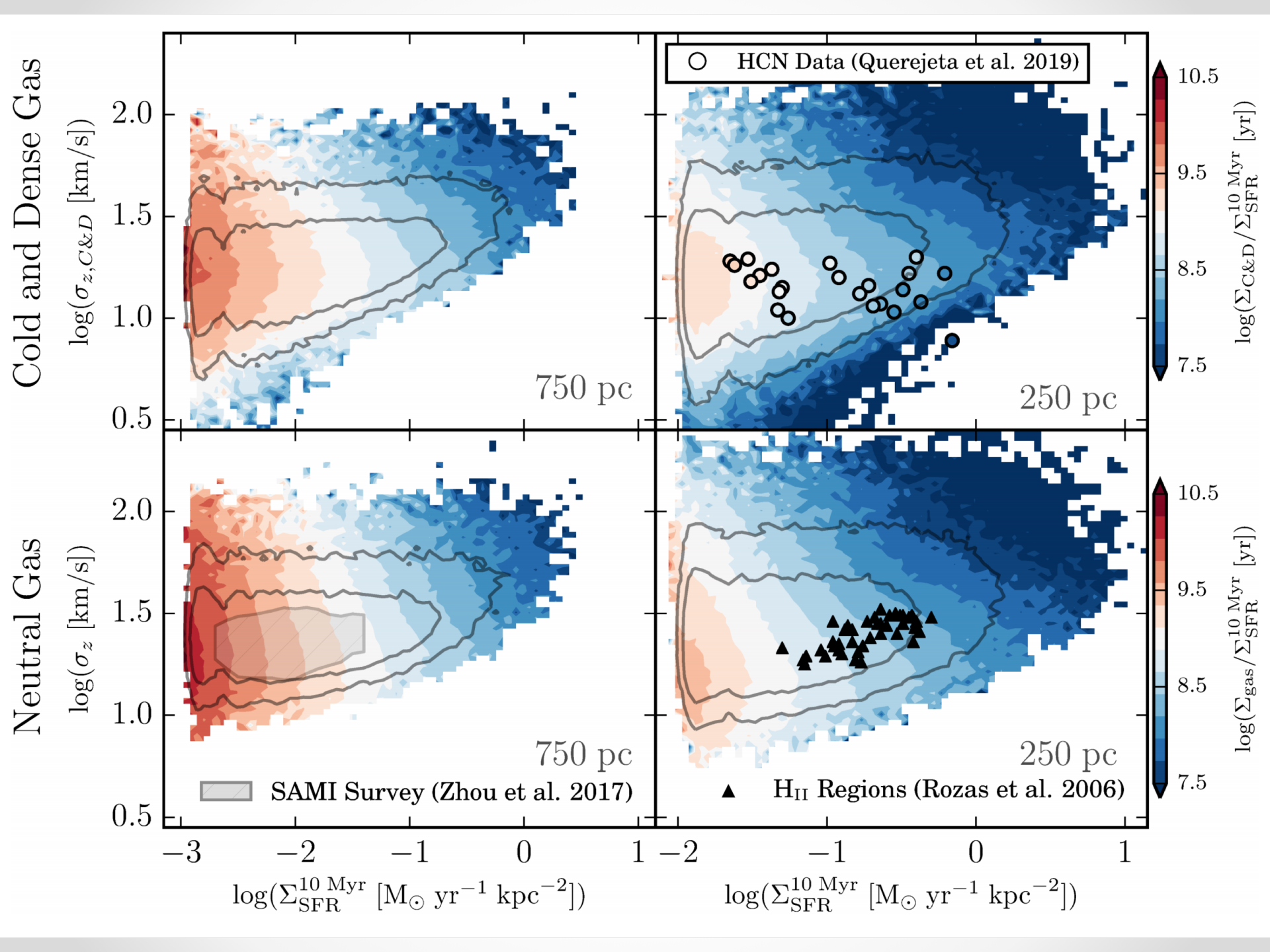
Cold and Dense Gas
Neutral Gas
HCN Data (Querejeta et al. 2019)
SAMI Survey (Zhou et al. 2017)
HII Regions (Rozas et al. 2006)
750 pc
250 pc
log(σz,C&D [km/s])
log(σz [km/s])
log(ΣSFR10 Myr [M⊙ yr−1 kpc−2])
log(ΣC&D/ΣSFR10 Myr [yr])
log(Σgas/ΣSFR10 Myr [yr])

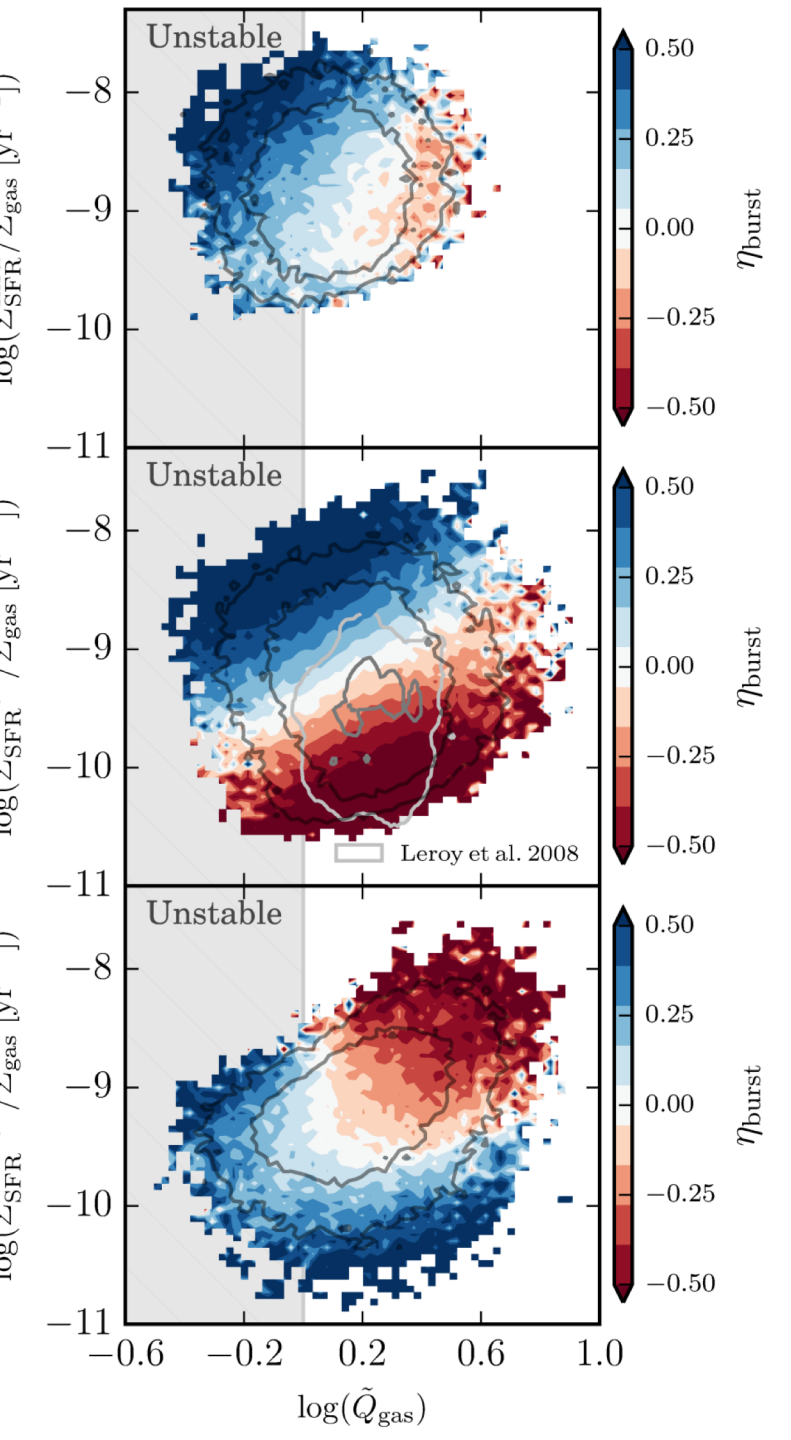
Unstable
Unstable
Unstable
Leroy et al. 2008
$\log(\tilde{Q}_{\rm gas})$
$\log(\Sigma_{\rm SFR}/\Sigma_{\rm gas}\ [{\rm yr}^{-1}])$
$\eta_{\rm burst}$
0.50
0.25
0.00
−0.25
−0.50

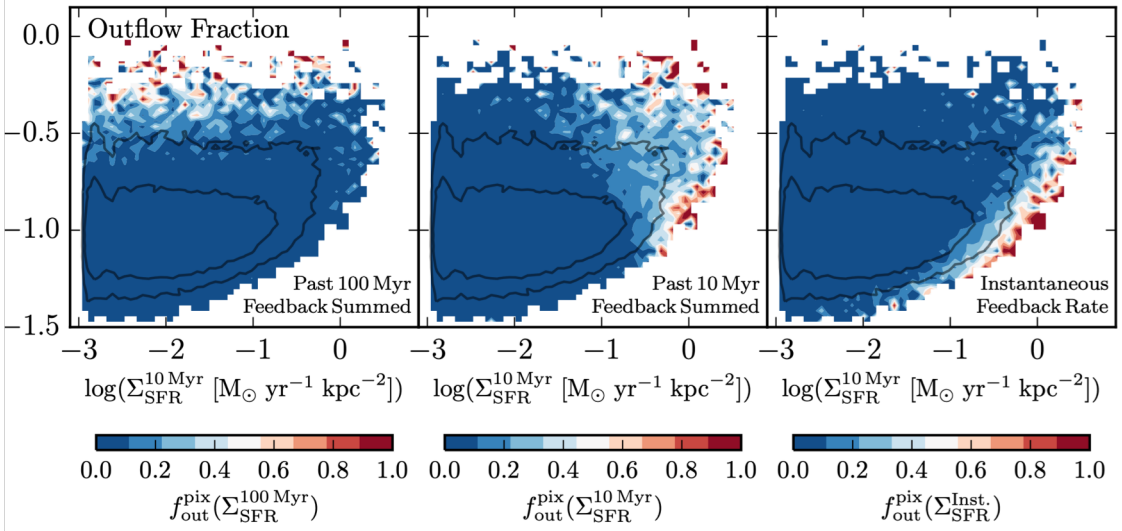
Outflow Fraction
Past 100 Myr Feedback Summed
Past 10 Myr Feedback Summed
Instantaneous Feedback Rate
$\log(\Sigma_{\rm SFR}^{10\,{\rm Myr}}\ [{\rm M}_\odot\ {\rm yr}^{-1}\ {\rm kpc}^{-2}])$
$f_{\rm out}^{\rm pix}(\Sigma_{\rm SFR}^{100\,{\rm Myr}})$
$f_{\rm out}^{\rm pix}(\Sigma_{\rm SFR}^{10\,{\rm Myr}})$
$f_{\rm out}^{\rm pix}(\Sigma_{\rm SFR}^{\rm Inst.})$

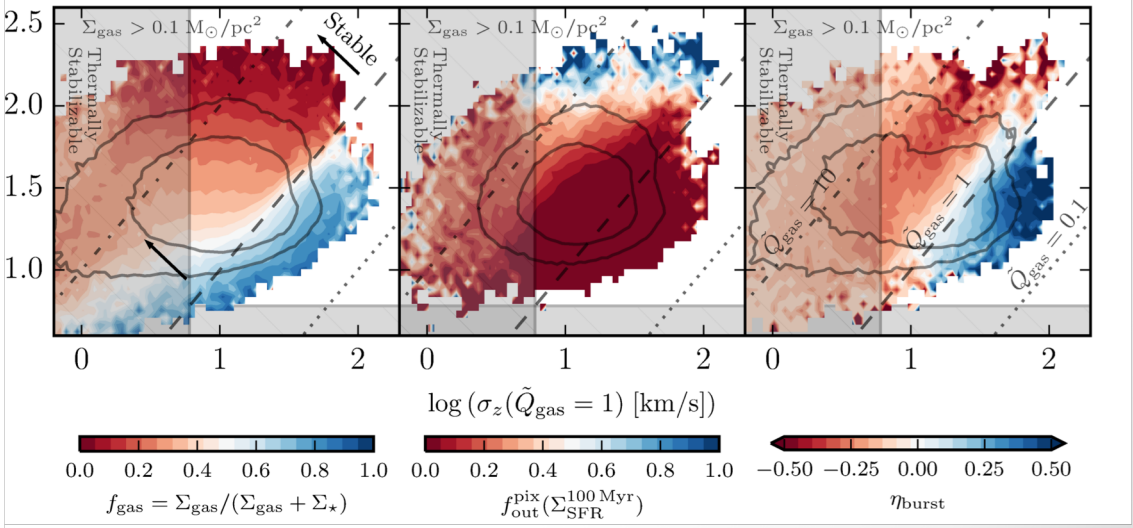
$\Sigma_{\rm gas} > 0.1\ {\rm M}_\odot/{\rm pc}^2$
Thermally Stabilizable
Stable
$\tilde{Q}_{\rm gas} = 10$
$\tilde{Q}_{\rm gas} = 1$
$\tilde{Q}_{\rm gas} = 0.1$
$\log\,(\sigma_z(\tilde{Q}_{\rm gas} = 1)\ [{\rm km/s}])$
$f_{\rm gas} = \Sigma_{\rm gas}/(\Sigma_{\rm gas} + \Sigma_\star)$
$f_{\rm out}^{\rm pix}(\Sigma_{\rm SFR}^{100\,{\rm Myr}})$
$\eta_{\rm burst}$

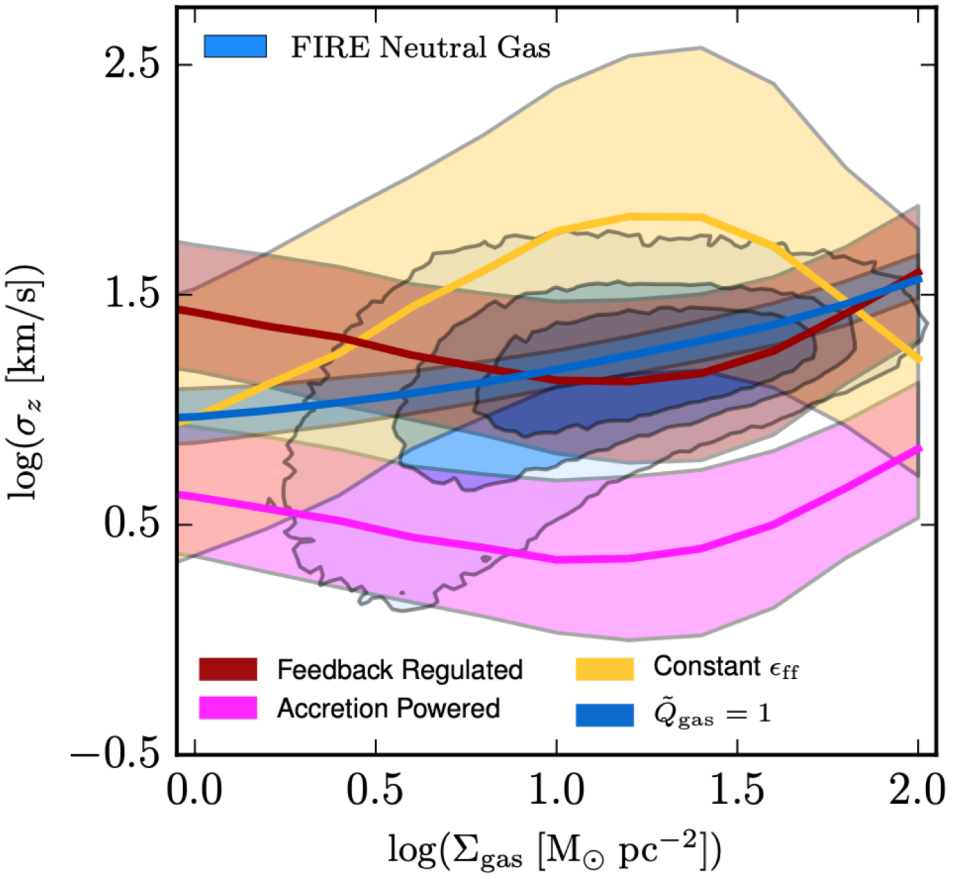

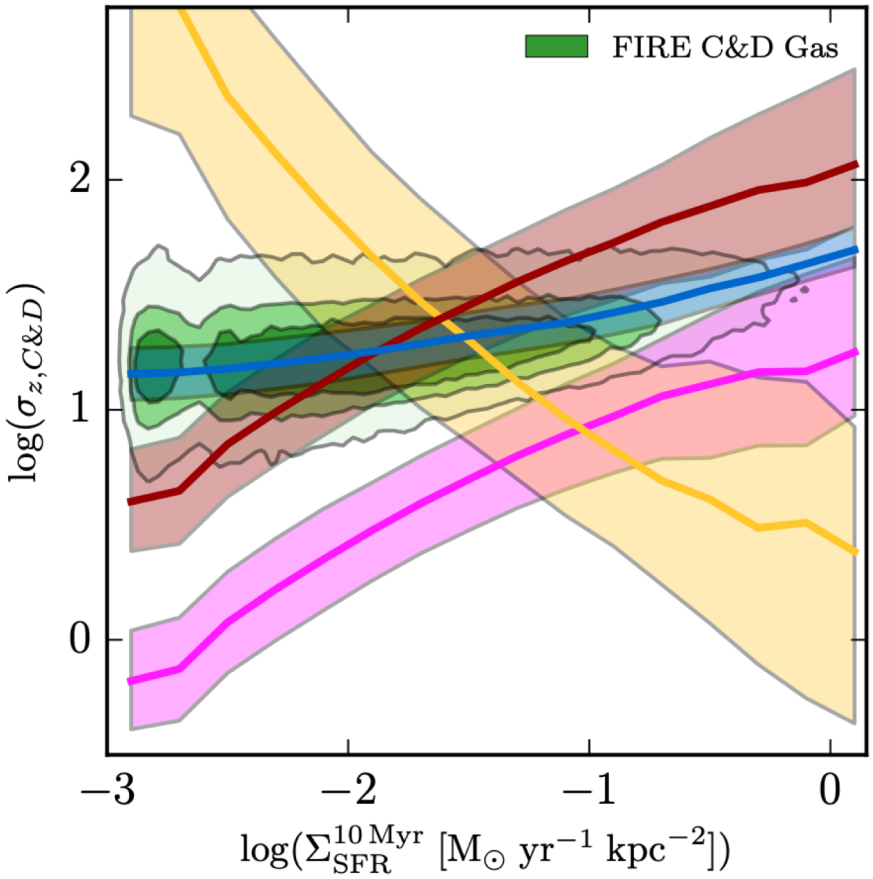

$$\sigma_{z,(Q=1)} = \frac{\pi G(\Sigma_{\rm gas} + \gamma\Sigma_\star)}{\sqrt{2}\Omega} \,.$$

$$\sigma_{z,CE} \approx \frac{32G}{3\pi}\epsilon_{\rm ff}^2 \frac{\Omega\Sigma_{\rm gas}^2\Sigma_{\rm disk}}{\Sigma_{\rm SFR}^2} \,.$$

$$\sigma_{z,FB} \approx \frac{2}{\sqrt{3}}(P/m_\star)\frac{\Sigma_{\rm SFR}}{\Omega\Sigma_{\rm gas}} \,.$$

$$\sigma_{z,AP} \approx \frac{\beta f}{\psi} v_c \frac{\Sigma_{\rm SFR}}{\Omega\Sigma_{\rm gas}} \,.$$